Optimizing Parameters on Nanophotocatalytic Degradation of Ibuprofen Using UVC/ZnO Processes by Response Surface Methodology

Noushin Rastkari[1], Akbar Eslami[2], Simin Nasseri[1], Ehsan Piroti[3], Anvar Asadi[4]*

[1]Center for Water Quality Research, Institute for Environmental Research,
Tehran University of Medical Sciences, Tehran, Iran
[2]Environmental and Occupational Hazards Control Research Center, Shahid Beheshti University
of Medical Sciences, Tehran, Iran
[3]Department of Environmental Health Engineering, School of public Health, Student Research Office,
Shahid Beheshti University of Medical Sciences, Tehran, Iran
[4]Research Center for Environmental Determinants of Health (RCEDH), Kermanshah University
of Medical Sciences, Kermanshah, Iran

Abstract

Due to the increasing importance of low-concentrated pollution of water resources, the photocatalytic decomposition of ibuprofen down to low ppm concentrations over zinc oxide catalyst has been studied. The aim of this work was to evaluate the degradation of the non-steroidal anti-inflammatory drug (NSAID) ibuprofen (IBP) using heterogeneous ZnO photocatalyst under UV-C irradiation. The photo catalyst was characterized by field emission scanning electron microscope (FE-SEM) and x-ray diffraction (XRD). The photocatalytic activity of ZnO nanoparticle was evaluated in a cylindrical glass reactor under VU-C irradiation light. Central composite design (CCD) and response surface methodology (RSM) were employed for modeling and optimizing the IBP degradation under different variables such as initial pH, ZnO loading, humic acid concentration, initial IBP concentration, and reaction time. The results of our experiments showed that the reaction time had its highest positive effect on IBP degradation. The correlation coefficient (R^2) value of 0.856 indicated a good agreement between the experimental results and the model predictions. Optimization results showed that the maximum IBP degradation was attained at optimum conditions of pH 6.7, catalyst loading 583 mg/L, initial IBP concentration 1.5 mg/L, humic acid concentration 54 mg/L, and reaction time of 95 min. Under these conditions we achieved maximum IBP removal efficiency of 82.97%. In conclusion, ZnO was found to be an effective photo catalyst and a promising alternative for producing free OH radicals for degradation of ibuprofen as an emerging pollutant in water resources.

Keywords: photocatalysis, ZnO nanoparticles, Ibuprofen, response surface methodology
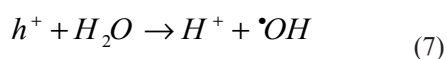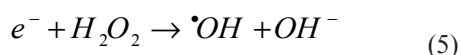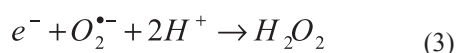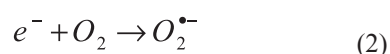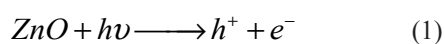
*e-mail: anvarasadi@sbmu.ac.ir

Introduction

The widespread use of hazardous pharmaceuticals has led to increasing pollution of surface, ground, and drinking water by these substances at low concentrations. Among pharmaceuticals, steroids, nonprescription drugs, and antibiotics occur at higher concentrations in aqueous environments [1]. Non-steroidal anti-inflammatory drugs (NSAIDs) such as ibuprofen, naproxen, diclofenac, and ketoprofen are the most frequently detected medicines, and their environmental distribution is widespread [2]. Based on selected characteristic properties, these drugs have the ability to be persistent during conventional treatment and release to the environment [2].

Most recently, several physical and chemical remediation technologies such as advanced oxidation processes (AOPs), filtration, adsorption, coagulation-flocculation, and flotation have been reported for the removal of NSAIDs from water and wastewaters [3-5]. AOPs as an environmentally friendly and green technology produce a very powerful oxidizing agent, hydroxyl radical •OH, which appears to be an alternative for the degradation of NSAIDs – especially at low concentrations [6]. One of the AOPs is the heterogeneous photocatalysis process, which use semiconductors such as ZnO, CdS, and TiO_2 under UV/visible light as a powerful technique for removing recalcitrant organic pollutants [7-8]. The ZnO semiconductor is comprised of a valence band and conductance band which under illumination higher than band gap produces electron-hole pairs (h^+/e^-) and is transferred to the ZnO surface, where they are then available to undergo redox reactions with substrates [9]. The following series of elementary reaction steps (Eqs. 1-8) are a simplified for reactions involving ZnO [10]:

$$ZnO + h\upsilon \longrightarrow h^+ + e^- \qquad (1)$$

$$e^- + O_2 \rightarrow O_2^{\bullet -} \qquad (2)$$

$$e^- + O_2^{\bullet -} + 2H^+ \rightarrow H_2O_2 \qquad (3)$$

$$O_2^{\bullet -} + H_2O_2 \rightarrow {}^{\bullet}OH + OH^- + O_2 \qquad (4)$$

$$e^- + H_2O_2 \rightarrow {}^{\bullet}OH + OH^- \qquad (5)$$

$$h^+ + OH^- \rightarrow {}^{\bullet}OH \qquad (6)$$

$$h^+ + H_2O \rightarrow H^+ + {}^{\bullet}OH \qquad (7)$$

$$2h^+ + 2H_2O \rightarrow 2H^+ + H_2O_2 \qquad (8)$$

Therefore, in heterogeneous photocatalysis several oxidative agents could be produced: the photogenerated holes h^+, •OH radicals, $O_2^{\bullet -}$ radicals, and H_2O_2 – which are known as strongly active and degrading agents [11].

The aim of the present study was to evaluate the potential of a UV/ZnO process for treatment of waters contaminated by IBP, using RSM with considering operational parameters such as initial pH, catalyst loading, initial IBP concentration, humic acid concentration, and reaction time. The central composite design (CCD) has been used for optimizing and modeling ibuprofen removal from the aqueous matrix.

Materials and Methods

Material

Ibuprofen (>98% purity) was obtained from Hakim Pharmaceutical co., Tehran, Iran. Commercial standard zinc oxide powder (GR) was purchased from Nano Pars Spadana, Isfahan, Iran, and its chemical structure and other characteristics are presented in our previous work [12]. X-ray diffraction patterns of the catalyst were carried out at room temperature with a STOE (Darmstadt, Germany) diffractometer using Cu Kα radiation (λ= 1.54060 Å). Field emission scanning electron microscopy (FE-SEM, Hitachi S-4160, Japan) was used for the morphological characterization of the catalyst. Humic acid was obtained from Sigma-Aldrich Co., USA, and used without further purification.

Experimental Set-Up and Procedure

An aqueous solution of IBP was prepared by adding the appropriate amount of IBP to methanol and yielding 1000 mg/L stock solution. The desired IBP concentrations (1.5-13 mg/L) were prepared from stock by dilution in deionized water. To detect and quantify IBP, the range of concentrations in this study is higher than those typically detected in the water resources [11]. Photocatalytic experiments were carried out in a cylindrical glass reactor with workable area of 0.07×0.25 m, fitted in a cooling bath. A 125 W medium pressure Hg vapor lamp (UV-C) with peak intensity at 254 nm was positioned above the reactor. The total suspension volume was 250 ml. Prior to each run, the substrate was maintained stirringly in the dark for 20 min to ensure adsorption-desorption equilibrium. The suspension pH values were adjusted by 0.1 M NaOH and HCl. At a given time interval, 2 mL aliquots of the aqueous suspension was withdrawn and filtered through syringe filters (Ø = 0.22 μm) to remove the remaining ZnO nanoparticles. The concentration of IBP in the filtered sample was determined by HPLC (Knauer, Germany) at a wavelength of 230 nm. The mobile phase consisted of 70% acetonitrile (HPLC Grade, Merck) and 30% ultra-pure water controlled at pH 3 by phosphoric acid. The flow rate was 1.2 mL/min and the sample volume was 20 μL.

Experimental Design Based on CCD

RSM based on central composite design (CCD) as a widely used experimental design was used to optimize

Table 1. Predictor variables and their coded levels and actual values used for experimental design.

Variable	Real values of coded levels				
	$-\alpha$	-1	0	1	$+\alpha$
pH (x_1)	2	5	8	10	13
Catalyst loading (x_2)	93	300	450	600	807
IBP concentration (x_3)	1.5	5	7.5	10	13
Humic acid(x_4)	16	50	75	100	134
Time (x_5)	10	12	45	70	95

IBP degradation by photocatalysis. Design-Expert and Minitab 17 software were used to analyze the obtained experimental data. The effect of five independent variables (factors) influencing the photocatalytic IBP degradation was evaluated: pH, catalyst loading (mg/L), the initial IBP concentration (mg/L), humic acid concentration (mg/L), and reaction time (min). Each factor in the design was studied at three different levels (low (-1), average (0), high (1)). The ranges and the levels of these factors assessed in this study are presented in Table 1.

The experimental response (Y) was related to selected factors with full quadratic model in terms of coded variables as follows:

$$Y = b_0 - b_1x_1 + b_2x_2 - b_3x_3 - b_4x_4 + b_5x_5 - b_{12}x_1x_2 + b_{13}x_1x_3$$
$$- b_{14}x_1x_4 + b_{15}x_1x_5 + b_{23}x_2x_3 - b_{24}x_2x_4 + b_{25}x_2x_5 - b_{34}x_3x_4 + b_{35}x_3x_5$$
$$- b_{45}x_4x_5 - b_{11}x_1^2 - b_{22}x_2^2 + b_{33}x_3^2 - b_{44}x_4^2 - b_{55}x_5^2$$

$$(9)$$

...where Y is a response variable of IBP degradation efficiency, b_0 is an intercept, b_i the regression coefficients for linear effects, b_{ii} the regression coefficients for quadratic effects, b_{ij} the regression coefficients for interaction effects, and X_i are coded experimental levels of the variables. The quality of fitting the quadratic model was expressed by the coefficient of determination R^2. Data from the study were analyzed by the analysis of variance (ANOVA).

Results

General ZnO Characterization

The ZnO catalyst used in the present work was a yellowish-white color with a specific surface area of about 50 m²/g and 99.8% purity. The catalyst was activated at 200ºC for two hours. Fig. 1a illustrates the XRD pattern of pure ZnO nanoparticle. The catalyst has a wurtzite structure and their XRD peaks were in good agreement with the standard card for the hexagonal ZnO crystal (JCPDS 36-1451). The average dimension (D) of particles was calculated using Debye-Sherrer's formula [8] and found to be 28 nm. The morphologies of the catalyst were
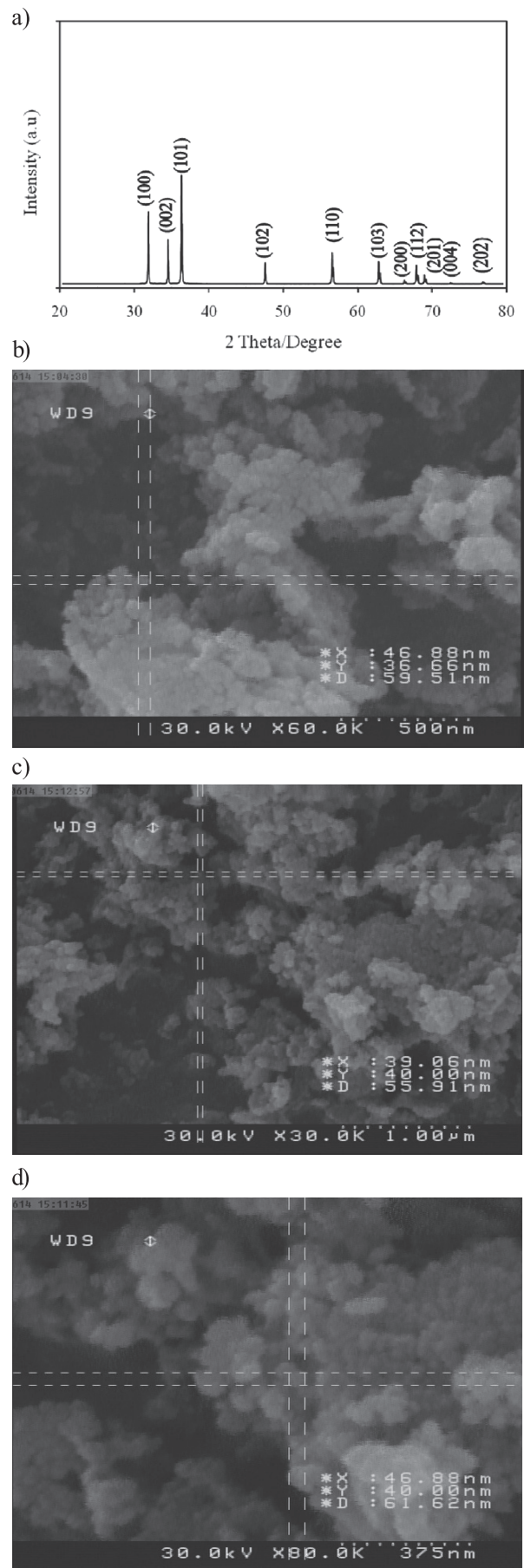

Fig. 1. a) XRD pattern of ZnO, and b), c), and d) FESEM images of ZnO at different magnifications.
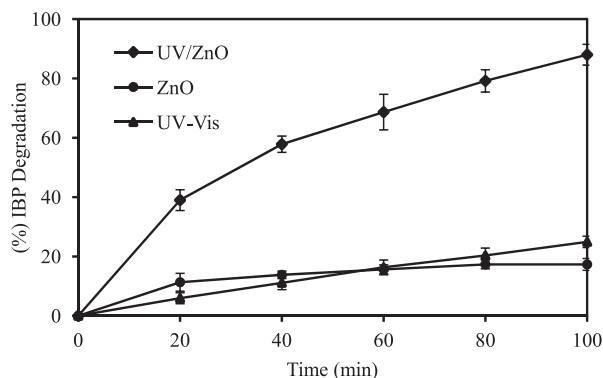
Fig. 2. Photocatalytic degradation of IBP over ZnO under different conditions: pH 7, catalyst load 500 mg/L, IPB concentration 5 mg/L, and Humic acid concentration 50 mg/L.

characterized by FE-SEM shown in Fig. 1 (b, c, and d). The approximate spherical shape of ZnO nanoparticles are observed in the figures. We can see that the size of the nanoparticles is between 25-35 nm, which is in agreement with particle diameters estimated by Debye-Sherrer's equation.

Preliminary Studies

Preliminary studies were performed to evaluate the effect of adsorption (pure ZnO), photolysis (UV irradiation alone), and photocatalyst (UV/ZnO) on IBP removal efficiency. The degradation curves of IBP as a function of reaction time are plotted in Fig. 2. From Fig. 2 it can be seen that adsorption and photolysis were contributed for 18 and 25% IBP removal, respectively, within 100 min of reaction time. Each factor alone could not have significant removal efficiency in this reaction time. On the other hand, the synergistic effect between the ZnO and UV light could effectively remove the IBP by photocatalysis (98% removal in 100 min reaction time). The results of these experiments are higher than a previous study by Choina

et al. [13], which reached 60% abatement of ibuprofen at 5 mg/L of IBP concentration. The finding is also in agreement with another study [11] on the photocatalytic (ZnO/UV) oxidation of ibuprofen, which obtained ca. 80% degradation in 10 mg/L IBP and catalyst loading of 50 mg/L.

Response Surface Methodology

Model Fitting and Statistical Analysis

To optimize IBP degradation, central composite design (CCD) with a total number of 50 runs was used for response surface modeling. The five-parameter CCD matrix and experimental results obtained in the photocatalytic IBP degradation runs are presented in Table 2. Design Expert software was used to obtain the best fitted model. As presented in Table 3, the quadratic model was suggested by the software and it was supported with lack of fit and model summary statistics.

Table 4 shows the results of the quadratic response surface model fitting in the form of analysis of variance (ANOVA).

Based on these results, RSM offers an empirical relationship between IBP degradation and independent variables as in the following quadratic model:

$$Y = +63.59 - 5.25x_1 + 4.78x_2 - 2.97x_3 - 1.88x_4 + 8.91x_5 - 2.63x_1x_2 + 0.77x_1x_3 \\ -0.58x_1x_4 + 2.47x_1x_5 + 0.45x_2x_3 - 0.093x_2x_4 + 0.60x_2x_5 - 0.63x_3x_4 + 0.54x_3x_5 \\ -0.82x_4x_5 - 5.29x_1^2 - 3.39x_2^2 + 1.55x_3^2 - 1.44x_4^2 - 1.36x_5^2$$

$$(10)$$

…where Y is the percentage degradation of IBP (%); and x_1, x_2, x_3, x_4, and x_5 are terms for the coded values of pH, catalyst loading (mg/L), IBP concentration (mg/L), humic acid concentration (mg/L), and time (min), respectively.

Table 5 shows the Student's t distribution and the corresponding values, along with the parameter estimate.

Table 2. Five-factor central composite design matrix along with the observed responses.

Run	pH	Cat. loading (mg/L)	IBP Con. (mg/L)	Humic acid con. (mg/L)	Time (min)	% IBP degradation	
						Observed	Predicted
1	8	450	7.5	75	10	31	37.2
2	10	600	5	50	45	44	58.5
3	8	450	7.5	134	70	53	53.5
4	10	300	5	100	45	38	42.4
5	8	450	7.5	75	12	32.5	37.9
6	10	600	5	100	45	51	52.9
7	5	300	10	50	95	58	67.4
8	5	600	10	50	95	78	78.0
9	13	450	7.5	75	70	42	53.5

Table 2. Continued.

10	5	300	5	100	45	61	48.0
11	10	300	10	100	95	56	56.2
12	5	300	5	50	45	55	53.6
13	10	600	5	100	95	66	72.0
14	10	300	5	50	45	49	47.9
15	10	600	5	50	95	71	77.6
16	8	450	7.5	75	70	59	60.2
17	5	300	5	50	95	65	72.7
18	10	300	5	100	95	64	61.5
19	10	600	10	50	95	73	72.4
20	8	450	7.5	75	70	58	60.2
21	8	807	7.5	75	70	70	72.7
22	10	300	10	50	95	70	61.8
23	10	300	10	50	45	40	42.7
24	8	450	7.5	75	70	60	60.2
25	8	450	7.5	16	70	69	66.8
26	5	600	10	50	45	64	58.8
27	8	450	7.5	75	70	60	60.2
28	2	450	7.5	75	70	38	66.8
29	5	600	5	50	45	70	64.1
30	10	600	10	100	45	34	47.6
31	5	300	5	100	95	60	67.1
32	8	450	7.5	75	70	77	60.2
33	10	300	10	100	45	40	37.1
34	10	600	10	50	45	44	53.2
35	8	450	1.5	75	70	79	66.5
36	5	300	10	100	95	55	61.9
37	8	93	7.5	75	70	30	47.6
38	10	600	10	100	95	65	66.8
39	5	600	5	100	45	64	58.5
40	8	450	7.5	75	70	81	60.2
41	10	300	5	50	95	74	67.1
42	5	300	10	100	45	45	42.7
43	5	600	10	100	95	70	72.4
44	5	600	10	100	45	58	53.2
45	8	450	7.5	75	70	80	60.2
46	5	600	5	100	95	76	77.7
47	8	450	7.5	75	70	83	60.2
48	5	300	10	50	45	48	48.3
49	5	600	5	50	95	83	83.2
50	8	450	13	75	70	78	54.4

Table 3. Sequential model fitting for IBP degradation.

Sequential Model Sum of Squares						
Source	Sum of Squares	df	Mean Square	F Value	p-value Prob > F	
Mean	176,358.6	1	176,358.6			
Linear	5,964.7	5	1,192.9	10.4	< 0.0001	
2FI	880.5	10	88.1	0.7	0.7015	
Quadratic	2,577.2	5	515.4	9.4	< 0.0001	Suggested
Cubic	552.6	16	34.5	0.4	0.9427	Aliased
Residual	1,037.7	13	79.8			
Total	187,371.3	50	3,747.4			
Lack of Fit Tests						
Source	Sum of Squares	df	Mean Square	F Value	p-value Prob > F	
Linear	4,144.4	37	112.0	0.9	0.6469	
2FI	3,263.9	27	120.9	0.9	0.5897	
Quadratic	686.7	22	31.2	0.2	0.9952	Suggested
Cubic	134.2	6	22.4	0.2	0.9758	Aliased
Pure Error	903.5	7	129.1			
Model Summary Statistics						
Source	Std. Dev.	R^2	Adjusted R^2	Predicted R^2	PRESS	
Linear	10.7	0.542	0.490	0.428	6298	
2FI	11.1	0.622	0.455	0.458	5973	
Quadratic	7.4	0.856	0.756	0.630	4071	Suggested
Cubic	8.9	0.906	0.645		+	Aliased

Graphical Presentation of the Model and Optimization

The study of the response surface and contour graphs provides a prediction of IBP removal efficiency and identifies the type of interactions between variables [14-16]. Figs. 3-6 show the response surface plots and contours for the optimization of IBP degradation. Indeed, the results of the interactions between the four independent variables and the dependent variable are shown in Figs 3-6. In each plot, two variables are varied while the others are maintained at their respective zero level. Fig. 3 shows the simultaneous effect of pH and catalyst loading. The degree of degradation increased with increasing catalyst load up to ~500 mg/L and then decreased.

Table 4. Analysis of variance (ANOVA) for the selected quadratic model.

Source	Sum of Squares	df	Mean Square	F Value	p-value Prob > F	
Model	9,422.4	20	471.1	8.6	< 0.0001	significant
Residual	1,590.2	29	54.8			
Lack of Fit	686.7	22	31.2	0.2	0.9952	not significant
Pure Error	903.5	7	129.1			
Cor Total	11,012.6	49				

Table 5. Regression results from the data of central composite design experiments.

Term	Effect	Coefficient Estimate	SE Coef.	T-Value	P-Value
Constant		62.78	2.46	25.56	0.000
X_1	-25.1	-12.55	3.41	-3.68	0.001
X_2	22.3	11.16	3.4	3.28	0.003
X_3	-15.1	-7.58	3.31	-2.29	0.029
X_4	-9.0	-4.52	3.4	-1.33	0.194
X_5	43.3	21.69	2.57	8.43	0.000
X_1^2	-57.5	-28.76	5.53	-5.2	0.000
X_2^2	-37.4	-18.72	5.52	-3.39	0.002
X_3^2	12.7	6.36	5.46	1.16	0.254
X_4^2	-15.4	-7.72	5.52	-1.4	0.173
X_5^2	-16.5	-8.26	3.16	-2.62	0.014
$X_1 \times X_2$	-35.0	-17.51	7.28	-2.41	0.023
$X_1 \times X_3$	7.8	3.93	7.04	0.56	0.581
$X_1 \times X_4$	-6.7	-3.36	7.28	-0.46	0.648
$X_1 \times X_5$	30.9	15.05	5.2	2.89	0.007
$X_2 \times X_3$	5.1	2.56	7.03	0.36	0.718
$X_2 \times X_4$	-1.0	-0.53	7.27	-0.07	0.942
$X_2 \times X_5$	6.8	3.41	5.2	0.66	0.517
$X_3 \times X_4$	-7.18	-3.59	7.03	-0.51	0.614
$X_3 \times X_5$	6.11	3.05	5.03	0.61	0.548
$X_4 \times X_5$	-9.35	-4.67	5.2	-0.9	0.376

Fig. 3. The counter plot and corresponding response surface plot of IBP degradation as a function of pH and catalyst loading (mg/L).

Fig. 4. Shows the simultaneous effect of IBP concentration and catalyst loading.

Figs 5 and 6 show the simultaneous effects of IBP vs. humic acid concentration and time vs. humic acid, respectively. As can be seen from Fig. 6, the degradation of IBP increased with increasing reaction time.

To optimize the operational parameters for maximum degradation efficiency, the operational factors were set to values within the studied range, whereas the response (IBP degradation efficiency) was set to achieve a maximum value. Based on this approach, maximum degradation efficiency was 90.4% at an initial pH of 6.7, catalyst loading of 583 mg/L, initial IBP concentration of 1.5 mg/L, initial humic acid concentration of 54 mg/L, and reaction time of 95 min. For validation study of optimal variables, additional experiments were carried out to confirm degradation efficiency. The result of optimization performed by Minitab 16 software showed that under optimal conditions the maximum degradation of 82.97% was obtained experimentally. This indicated the suitability and accuracy of the model.
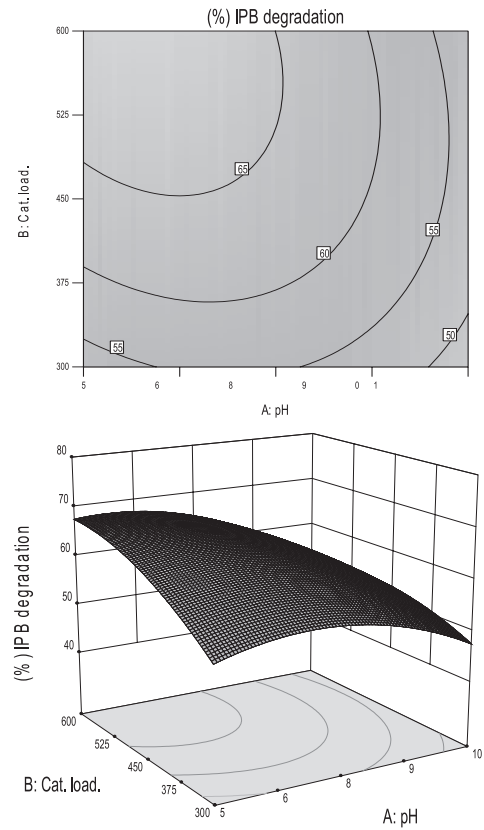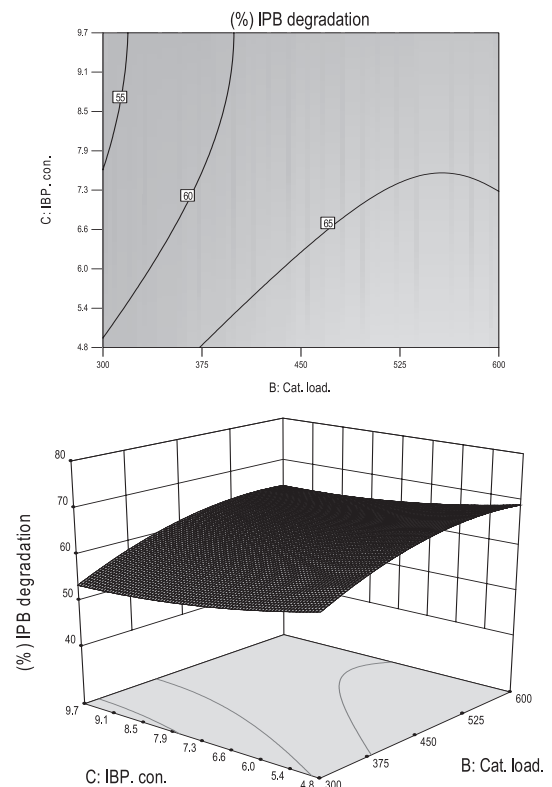

Fig. 4. The counter plot and corresponding response surface plot of IBP degradation as a function of catalyst loading (mg/L) and initial IBP concentration (mg/L).
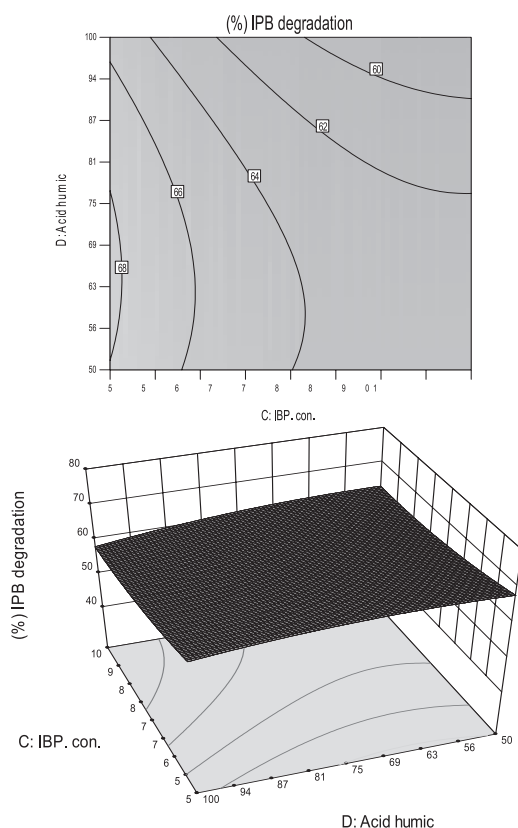
Fig. 5. The counter plot and corresponding response surface plot of IBP degradation as a function of initial IBP concentration (mg/L) and humic acid concentration (mg/L).
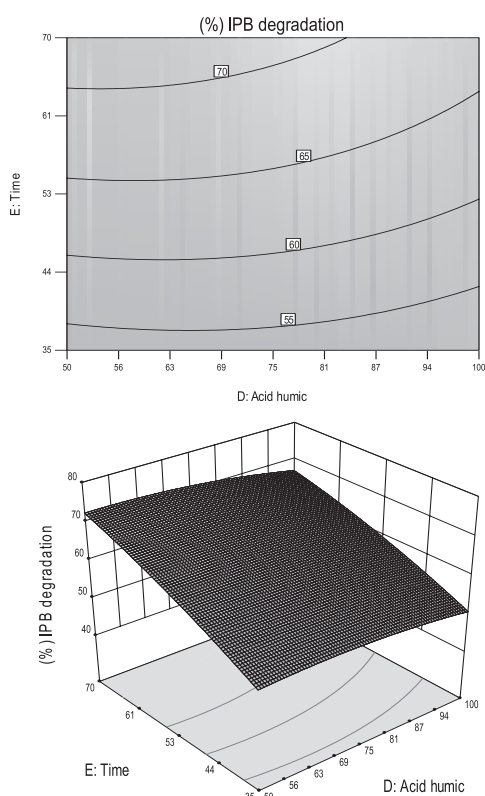

Fig. 6. The counter plot and corresponding response surface plot of IBP degradation as a function of time (min) and humic acid concentration (mg/L).

Discussion

The ANOVA of the quadratic regression model indicates that the model is highly significant, as is evident from the Fisher F-test (F model = 8.59) and a very low p-value prob>F (< 0.0001). The probability P-value is relatively low, indicating the significance of the model. The tabular F-value ($F_{0.05, 5, 44}$ = 2.43) is much lower than the computed F-value (8.59) at the 1% level, which indicates the great significance of IBP degradation. The lack of fit of the model occurs when the model does not adequately represent the mean response as a function of the factor levels. Here, the lack of fit value is 0.241, which indicates that the lack of fit is not significant relative to the pure error when p = 0.995, which is > 0.05. The insignificant lack of fit indicates good predictability. The model fitting could be also checked by the coefficient of determination, which lies between 0 and 1. The value of R^2 is 0.855, which indicates that 85.5% of the variability in the response could be explained by quadratic model. To correct the number of factors in the model and sample size, the adjusted R^2 could be used. However, adding a variable to the model could always increase R^2, regardless of whether or not the additional variables are statistically significant [14]. Thus, some researchers prefer to use adjusted R^2. When variables are added to the model, the adjusted R^2 will not necessarily increase. In fact, if unnecessary variables are added to the model, the value of adjusted R^2 is often decreasing. Large differences between R^2 and adjusted R^2 mean that insignificant variables are included in the model. Here, an adjusted R^2 value 0.75 was relatively close to R^2 value.

We used P-values o check the significance of each of the coefficients and as well as understand the pattern of the mutual interactions between the independent variables. The larger the magnitude of the t-value and smaller the P-value, the more significant the corresponding coefficient [15]. As can be seen from Table 5, the linear effect of all terms (with the exception of humic acid concentration) is significant at 5% significance level (95% confidence interval). The quadratic relations between pH, catalyst loading, and time were also significant. The mutual interaction effect of pH*catalyst loading and pH*time were significant, which indicated that these interactions improve IBP degradation efficiency. From the values of the coefficients in the regression model, the order in which independent variables effect the response is, time (x_5) > pH (x_1) > catalyst loading (x_2) > IBP concentration (x_3) > humic acid concentration (x_4). However, some terms such as pH, IBP concentration, and humic acid concentration have a negative effect on response.

In Fig. 3, a preliminary increase in degradation with increasing catalyst load can be related to the increase in the amount of photon absorption on the catalyst surface, availability of active sites on ZnO surface, and light penetration of photo-activating light into the suspension, which promotes degradation efficiency. The decrease in degradation from a certain catalyst load may be due to increased opacity of the suspension and also increased

light reflectance as a consequence of surplus ZnO particles [17]. The involved reactions in the ZnO photocatalyst system for removal of IBP as an organic pollutant are described before in equations 1 to 8. However, when the ZnO semiconductor is illuminated with light energy greater than its band gap energy, excited high-energy states of electron (e$^-$) and hole (h$^+$) pairs are produced [18]. Electrons (e$^-$) are trapped by surface O_2 to produce the superoxide radicals ($O_2^{\bullet-}$), and also react with $O_2^{\bullet-}$ to produce H_2O_2. The superoxide radicals can combine with H_2O_2 to produce the $^{\bullet}OH$ radicals. Electrons (e$^-$) can react with H_2O_2 and produce $^{\bullet}OH$ radicals. Holes (h$^+$) are combined with ^-OH and H_2O and produce $^{\bullet}OH$ radicals and H_2O_2. All of h$^+$, $O_2^{\bullet-}$, H_2O_2, and $^{\bullet}OH$ are reactive species responsible for the oxidizing ibuprofen [19]. pH has an important effect on the removal of IBP by the UV/ZnO process. Apparently, the circumneutral condition is most favorable for IBP degradation by ZnO. It has been reported that the pH of zero point charge for ZnO is 9.0 [20]. At pH value below the point of zero charge the catalyst surface becomes protonated and gets positive charge and at higher pH becomes deprotonated and get a negative charge. On the other hand, IBP is a weak acid that has a PKa value of 4.4. Therefore, the optimal degradation of IBP occurs at $PK_a^{IBP} < pH < pH_{PZC}^{ZnO}$, of which ZnO has a positive charge and IBP molecule get a negative charge [1, 21].

Based on Fig. 4, the degradation of IBP decreases with increasing IBP concentration. As initial IBP concentration decreases, more hydroxyl radicals ($^{\bullet}OH$) are available to remove the IBP, which in turn leads to increasing IBP degradation efficiency [22].

To evaluate the effect of natural organic matter (NOM) on IBP degradation, humic acid was selected as a model of NOM since NOM is comprised of ~70% humic acid [23]. As depicted in Fig. 5, the degradation of IBP diminishes with increasing humic acid concentration. However, as discussed earlier, at this level of humic acid concentration there is no significant effect on IBP degradation. Finally, Fig. 6 showed the effect of time and humic acid on IBP degradation. It can be seen that the large amount of IBP is degraded in the first 30 min of photocatalytic treatment. The rate of degradation decreased with increasing time above 30 min, which related to a deactivation of the catalyst during the course of reaction. These results are in agreement with Sheikhnejad-Bishe et al. [24], which evaluated the effect of TiO_2 nanoparticles synthesized via low temperature on the degradation of methyl orange under a 150 W xenon lamp.

Conclusions

The modeling and optimization of photocatalytic degradation of IBP in the UVC/ZnO process was investigated using an RSM. The results showed that the optimum removal was occurring at the circumneutral pH condition. The amount of IBP degradation increased with initial concentration of the photocatalyst. A central composite design was used to develop a second-order polynomial model as a function of IBP removal and the five independent variables. The optimized factors for IBP removal determined in this work were set as follows: initial pH of 6.7, catalyst loading of 583 mg/L, initial IBP concentration of 1.5 mg/L, initial humic acid concentration of 54 mg/L, and reaction time of 95 min. At this condition we obtained 82.97% removal of IBP.

Acknowledgements

References

1. CHOINA J., KOSSLICK H., FISCHER C., FLECHSIG G.U., FRUNZA L., SCHULZ A. Photocatalytic decomposition of pharmaceutical ibuprofen pollutions in water over titania catalyst. Applied Catalysis B: Environmental **129**, 589, **2013**.
2. ESLAMI A., AMINI M.M., YAZDANBAKHSH A.R., RASTKARI N., MOHSENI-BANDPEI A., NASSERI S., PIROTI E., ASADI A. Occurrence of non-steroidal anti-inflammatory drugs in Tehran source water, municipal and hospital wastewaters, and their ecotoxicological risk assessment. Environmental monitoring and assessment **187**, 1, **2015**.
3. MÉNDEZ-ARRIAGA F., ESPLUGAS S., GIMÉNEZ J. Photocatalytic degradation of non-steroidal anti-inflammatory drugs with TiO_2 and simulated solar irradiation. Water Research **42**, 585, **2008**.
4. CARBALLA M., OMIL F., LEMA J.M. Removal of cosmetic ingredients and pharmaceuticals in sewage primary treatment. Water Research **39**, 4790, **2005**.
5. ZIYLAN A., INCE N.H. The occurrence and fate of anti-inflammatory and analgesic pharmaceuticals in sewage and fresh water: Treatability by conventional and non-conventional processes. Journal of Hazardous Materials **187**, 24, **2011**.
6. BAUER R., WALDNER G., FALLMANN H., HAGER S., KLARE M., KRUTZLER T., MALATO S., MALETZKY P. The photo-Fenton reaction and the TiO_2/UV process for waste water treatment− novel developments. Catalysis today **53**, 131, **1999**.
7. CHONG M.N., JIN B. Photocatalytic treatment of high concentration carbamazepine in synthetic hospital wastewater. Journal of Hazardous Materials **199-200**, 135, **2012**.
8. SALARIAN A.-A., HAMI Z., MIRZAEI N., MOHSENI S.M., ASADI A., BAHRAMI H., VOSOUGHI M., ALINEJAD A., ZARE M.-R. N-doped TiO_2 nanosheets for photocatalytic degradation and mineralization of diazinon under simulated solar irradiation: Optimization and modeling using a response surface methodology. Journal of Molecular Liquids **220**, 183, **2016**.
9. DAGHRIR R., DROGUI P., DIMBOUKOU-MPIRA A., EL KHAKANI M.A. Photoelectrocatalytic degradation of carbamazepine using Ti/TiO_2 nanostructured electrodes deposited by means of a pulsed laser deposition process. Chemosphere **93**, 2756, **2013**.

10. CHO M., CHUNG H., CHOI W., YOON J. Different inactivation behaviors of MS-2 phage and Escherichia coli in TiO_2 photocatalytic disinfection. Applied and environmental microbiology **71**, 270, **2005**.

11. GEORGAKI I., VASILAKI E., KATSARAKIS N. A Study on the Degradation of Carbamazepine and Ibuprofen by TiO_2 & ZnO Photocatalysis upon UV/Visible-Light Irradiation. **5**, 518, **2014**.

12. ASSADI A., DEHGHANI M.H., RASTKARI N., NASSERI S., MAHVI A.H. Photocatalytic reduction of hexavalent chromium in aqueous solutions with zinc oxide nanoparticles and hydrogen peroxide. Environment Protection Engineering **38**, 5, **2012**.

13. CHOINA J., BAGABAS A., FISCHER C., FLECHSIG G.U., KOSSLICK H., ALSHAMMARI A., SCHULZ A. The influence of the textural properties of ZnO nanoparticles on adsorption and photocatalytic remediation of water from pharmaceuticals. Catalysis Today **241, Part A**, 47, **2015**.

14. KUMAR J., BANSAL A. Photocatalytic degradation in annular reactor: Modelization and optimization using computational fluid dynamics (CFD) and response surface methodology (RSM). Journal of Environmental Chemical Engineering **1**, 398, **2013**.

15. LIU H.-L., CHIOU Y.-R. Optimal decolorization efficiency of Reactive Red 239 by UV/TiO_2 photocatalytic process coupled with response surface methodology. Chemical Engineering Journal **112**, 173, **2005**.

16. BOX G.E., DRAPER N.R. Empirical model-building and response surfaces, (Wiley New York, **1987**).

17. KURIECHEN S.K., MURUGESAN S., RAJ S.P., MARUTHAMUTHU P. Visible light assisted photocatalytic mineralization of Reactive Red 180 using colloidal TiO_2 and oxone. Chemical Engineering Journal **174**, 530, **2011**.

18. RADJENOVIĆ J., SIRTORI C., PETROVIĆ M., BARCELÓ D., MALATO S. Solar photocatalytic degradation of persistent pharmaceuticals at pilot-scale: Kinetics and characterization of major intermediate products. Applied Catalysis B: Environmental **89**, 255, **2009**.

19. ESLAMI A., AMINI M.M., YAZDANBAKHSH A.R., MOHSENI-BANDPEI A., SAFARI A.A., ASADI A. N,S co-doped TiO_2 nanoparticles and nanosheets in simulated solar light for photocatalytic degradation of non-steroidal anti-inflammatory drugs in water: a comparative study. Journal of Chemical Technology & Biotechnology, n/a, **2016**.

20. PARKS G.A. The isoelectric points of solid oxides, solid hydroxides, and aqueous hydroxo complex systems. Chemical Reviews **65**, 177, **1965**.

21. DANESHVAR N., ABER S., SEYED DORRAJI M.S., KHATAEE A.R., RASOULIFARD M.H. Photocatalytic degradation of the insecticide diazinon in the presence of prepared nanocrystalline ZnO powders under irradiation of UV-C light. Separation and Purification Technology **58**, 91, **2007**.

22. KHATAEE A.R., ZAREI M., ASL S.K. Photocatalytic treatment of a dye solution using immobilized TiO_2 nanoparticles combined with photoelectro-Fenton process: optimization of operational parameters. Journal of Electroanalytical Chemistry **648**, 143, **2010**.

23. BEHERA S., OH S., PARK H. Sorptive removal of ibuprofen from water using selected soil minerals and activated carbon. International journal of environmental science and technology **9**, 85, **2012**.

24. SHEIKHNEJAD-BISHE O., ZHAO F., RAJABTABAR-DARVISHI A., KHODADAD E., HUANG Y. Precursor and Reaction Time Effects in Evaluation of Photocatalytic Properties of TiO_2 Nanoparticles Synthesized via Low Temperature. Int. J. Electrochem. Sci **9**, 3068, **2014**.